Maternal stress programs accelerated aging of the basal ganglia motor system in offspring

Jordan Marrocco, Remy Verhaeghe, Domenico Bucci, Luisa Di Menna, Anna Traficante, Hammou Bouwalerh, Gilles van Camp, Veronica Ghiglieri, Barbara Picconi, Paolo Calabresi, et al.

HAL Id: hal-03179221

https://hal.univ-lille.fr/hal-03179221v1

Submitted on 24 Mar 2021

Maternal stress programs accelerated aging of the basal ganglia motor system in offspring

Jordan Marrocco [a,1,3], Remy Verhaeghe [b,1], Domenico Bucci [b], Luisa Di Menna [b], Anna Traficante [b], Hammou Bouwalerh [c,m], Gilles Van Camp [c,m], Veronica Ghiglieri [d,e], Barbara Picconi [f], Paolo Calabresi [g], Laura Ravasi [h], Francesca Cisani [c,i], Farzaneh Bagheri [c,n], Anna Pittaluga [i,j], Valeria Bruno [b,k], Giuseppe Battaglia [b,k], Sara Morley-Fletcher [c,m], Ferdinando Nicoletti [b,k,2], Stefania Maccari [c,l,*,2]

[a] Harold and Margaret Milliken Hatch Laboratory of Neuroendocrinology, The Rockefeller University, 10065, NY, USA
[b] IRCCS Neuromed, Località Camerelle, 86077, Pozzilli, Italy
[c] Univ. Lille, CNRS, UMR 8576 - UGSF - Unité de Glycobiologie Structurale et Fonctionnelle, F-59000, Lille, France
[d] IRCCS Santa Lucia Foundation, Laboratory of Neurophysiology, via del Fosso di Fiorano, 64, 00143, Rome, Italy
[e] Department of Medicine, University of Perugia, Italy
[f] Laboratory of Experimental Neurophysiology, IRCCS San Raffaele Pisana, Rome, Italy
[g] Neurologia, Fondazione Policlinico Universitario Agostino Gemelli IRCCS, Piazzale Agostino Gemelli 8, 00168, Rome, Italy
[h] EA1046, IMPRT-IFR114, Faculty of Medicine, University of Lille, 59000, Lille, France
[i] Dept. of Pharmacology, School of Medical and Pharmaceutical Sciences, Center of Excellence for Biochemical Research (CEBR), University of Genova, Italy
[j] IRCCS San Martino Hospital Genova Italy, Italy
[k] Departments of Physiology and Pharmacology "V. Erspamer", University Sapienza of Rome, 00185, Rome, Italy
[l] Science and Medical - Surgical Biotechnology, University Sapienza of Rome, 00185, Rome, Italy
[m] International Associated Laboratory (LIA) "Perinatal Stress and Neurodegenerative Diseases": University of Lille - CNRS, UMR 8576, Sapienza University of Rome and IRCCS Neuromed, Italy
[n] School of Biology, Damghan University, Damghan, Iran

ARTICLE INFO

ABSTRACT

Early-life stress involved in the programming of stress-related illnesses can have a toxic influence on the functioning of the nigrostriatal motor system during aging. We examined the effects of perinatal stress (PRS) on the neurochemical, electrophysiological, histological, neuroimaging, and behavioral correlates of striatal motor function in adult (4 months of age) and old (21 months of age) male rats. Adult PRS offspring rats showed reduced dopamine (DA) release in the striatum associated with reductions in tyrosine hydroxylase-positive (TH$^+$) cells and DA transporter (DAT) levels, with no loss of striatal dopaminergic terminals as assessed by positron emission tomography analysis with fluorine-18-l-dihydroxyphenylalanine. Striatal levels of DA and its metabolites were increased in PRS rats. In contrast, D_2 DA receptor signaling was reduced and A_{2A} adenosine receptor signaling was increased in the striatum of adult PRS rats. This indicated enhanced activity of the indirect pathway of the basal ganglia motor circuit. Adult PRS rats also showed poorer performance in the grip strength test and motor learning tasks. The aged PRS rats also showed a persistent reduction in striatal DA release and defective motor skills in the pasta matrix and ladder rung walking tests. In addition, the old rats showed large increases in the levels of SNAP-25 and synaptophysin, which are synaptic vesicle-related proteins in the striatum, and in the PRS group only, reductions in Syntaxin-1 and Rab3a protein levels were observed. Our findings indicated that the age-dependent threshold for motor dysfunction was lowered in PRS rats. This area of research is underdeveloped, and our study suggests that early-life stress can contribute to an increased understanding of how aging diseases are programmed in early-life.

Abbreviations

PRS	perinatal stress
CONT	control
DA	dopamine
TH + cells	tyrosine hydroxylase positive cells
DAT	dopamine transporter
[^{18}F]-DOPA	fluorine-18-l-dihydroxyphenylalanine
PET	positron emission
D_1 DA receptor	Doamine receptor D_1
D_2 DA receptor	Dopamine receptor D_2
SNAP-25	Synaptosomal-Associated Protein, 25 kDa
SYP	synaptophysin
PD	Parkinson's Disease
L-DOPA	levodopa; L-3,4-dihydroxyphenylalanine
AA	active avoidance
CS	conditioned stimulus
US:	unconditioned stimulus
MSNs	medium spiny neurons
sEPSP	spontaneous excitatory postsynaptic potential
HFS	high-frequency stimulation
LTD	long-term depression
MRI	magnetic resonance imaging
ROIs	regions of interest
DOPAC	3,4-dihydroxyphenylacetic
HVA	homovanillic acid
HPLC	high-performance liquid chromatography
GABA	gamma-aminobutyric acid
IBMX	3-isobutyl-1-methylxanthine
$A_{2A}R$	adenosine A_{2A} receptor
EPM	elevated plus maze
RMP	resting membrane potential
NMDA/AMPA	N-methyl-D-aspartate/α-amino-3-hydroxy-5-methyl-4-isoxazolepropionic acid

1. Introduction

While the comorbidity between motor and stress-related disorders is well established (Laureti et al., 2016; Suguma et al., 2016), the nature of this association remains largely unexplored. In particular, little is known about how early-life stress, which predisposes to stress-related disorders, affects the development of the nigrostriatal system and the risk of age-related disorders. The neostriatum, the major input station of the basal ganglia motor circuit, is connected to output stations (the internal globus pallidus and *substantia nigra* pars reticulata) through direct and indirect pathways. Increased activity of the indirect pathway involving D_2 dopamine (DA) and A_{2A} adenosine receptors, as occurs in Parkinson's disease (PD), enhances the inhibitory control of the output stations on thalamocortical neurons. In contrast, increased activity of the direct pathway involving the D_1 receptors leads to exaggerated motor activity as in L-3,4-dihydroxyphenylalanine (L-DOPA)-induced dyskinesias (Conn et al., 2005; Cenci et al., 2009; Calabresi et al., 2014). Not surprisingly, most studies on stress and DA have focused on the mesolimbic system. However, changes in the activity of the direct and indirect pathways of the striatal motor circuit have been reported after exposure to uncontrollable stress (Clark et al., 2014), and changes in striatal DA levels are observed in response to chronic stress in adult rats (Ida et al., 1982). Early-life stress causes changes in DA turnover in the striatum, nucleus accumbens, and prefrontal cortex (Fride and Weinstock, 1988; Alonso et al., 1997), leading to a delay in motor development (Barlow et al., 1978).

The rat model of perinatal stress (PRS), in which exposure of pregnant dams to restraint stress reduces maternal behavior (Gatta et al., 2018), has face, construct, and pharmacological validity as an epigenetic model of stress-related disorders (Maccari et al., 2014). PRS alters the developmental trajectory of the offspring, causing long-lasting neurochemical, endocrine, and behavioral alterations (Maccari et al., 2017). These alterations are associated with large reductions in glutamate release and the expression of synaptic vesicle-associated proteins in the ventral hippocampus (Marrocco et al., 2012; Morley-Fletcher et al., 2018). PRS also affects the mesolimbic dopaminergic system, increasing amphetamine self-administration and hedonic sensitivity to natural rewards (Deminiere et al., 1992; Reynaert et al., 2016). There are only a few studies on how early-life stress programs the activity of the basal ganglia motor circuit in adult life. For example, PRS has been shown to affect the symmetry of D_2 receptor expression in the medial caudate-putamen (Adrover et al., 2007), attenuate haloperidol-induced catalepsy, and enhance apomorphine-induced stereotypies (Marrocco et al., 2013). However, no studies have been performed in old rats, despite a well-known decline in mobility with age and the identification

of age as a risk factor for motor disorders, as observed in PD. Therefore, we examined whether PRS causes long-lasting changes in striatal motor programming and whether some of these changes persist during aging.

2. Materials and methods

2.1. Experimental design

The experimental timelines are shown in Fig. 1. After the PRS procedure, consisting of restraint stress on the pregnant dams and reduced maternal behavior in the first postpartum week, behavioral and biochemical examinations of the striatum of adult (3–5 months of age) and aged (21 months of age) male progeny were performed. All experiments followed the rules of the European Communities Council Directive 86/609/EEC. The Local Committee CEEA-75 (Comité d'Ethique en Experimentation Animale Nord-Pas de Calais, 75) approved the experimental protocol.

2.2. Animals

Ninety nulliparous female Sprague–Dawley rats, weighing approximately 250 g each, were purchased from Charles River (France) and housed under standard conditions with a 12-h light/dark cycle. After group housing (5 females/cage) for two weeks, each female was individually housed for one week with a sexually experienced male rat. Following this, a gain of at least 10 g was considered an indication of pregnancy.

2.3. Stress procedure

The stress procedure was performed on three separate sets of pregnant rats, each set comprising 30 females (15 control and 15 stressed dams). PRS procedure, i.e., the adult offspring of dams that were exposed to multiple episodes of restraint stress during pregnancy causing reduced maternal care were obtained according to our standard protocol (Maccari et al., 1995), as shown in Fig. 1. Briefly, from day 11 of pregnancy until delivery, pregnant females were subjected to restraint in a transparent plastic cylinder and exposed to bright light during three daily sessions lasting 45 min each. Control pregnant females were left undisturbed in their home cages and handled weekly. After weaning, only male offspring from litters with a balanced sex ratio were used for the experiments. The animals were housed in groups of two or three and maintained under similar environmental conditions throughout their life span.

2.4. Behavioral studies

2.4.1. Two-way active avoidance test

Motor learning and locomotion were measured through a two-way active avoidance (AA) test by means of a shuttle-box. The AA test requires learning that an explicitly conditioned stimulus (CS, light) precedes the delivery of a negative unconditioned stimulus (US, foot shock). A shuttle box ($40 \times 10 \times 15$ cm) equipped with a transparent cover, light bulb, stainless-steel grid on the floor, and two communicating compartments was used. The rats were subjected to one AA session (duration, 30 min; 60 avoidance trials) for five consecutive days. Each trial consisted of 22 s of darkness followed by a 4-s light signal (CS) presented in one compartment and subsequently 4 s of light associated with an electric foot shock (0.2 mA, 25 s) in the same compartment (US). The number of conditioned responses in the AA test (crossings occurring within 8 s of CS), the average escape latency to cross to the other compartment after the start of each CS, and the number of inter-trial crossings between the two compartments were automatically recorded (Ugo Basile). Foot-shock sensitivity was evaluated by measuring pain thresholds with increasing current intensities (0–0.6 mA), with the minimal intensity eliciting vocalization and jumping retained as the score. Rats failing to squeak were given a maximum score of 0.6 mA.

Exp. 1: PRS effect on cortico-striatal transmission and nigro-striatal dopaminergic transmission and related behavior in adulthood
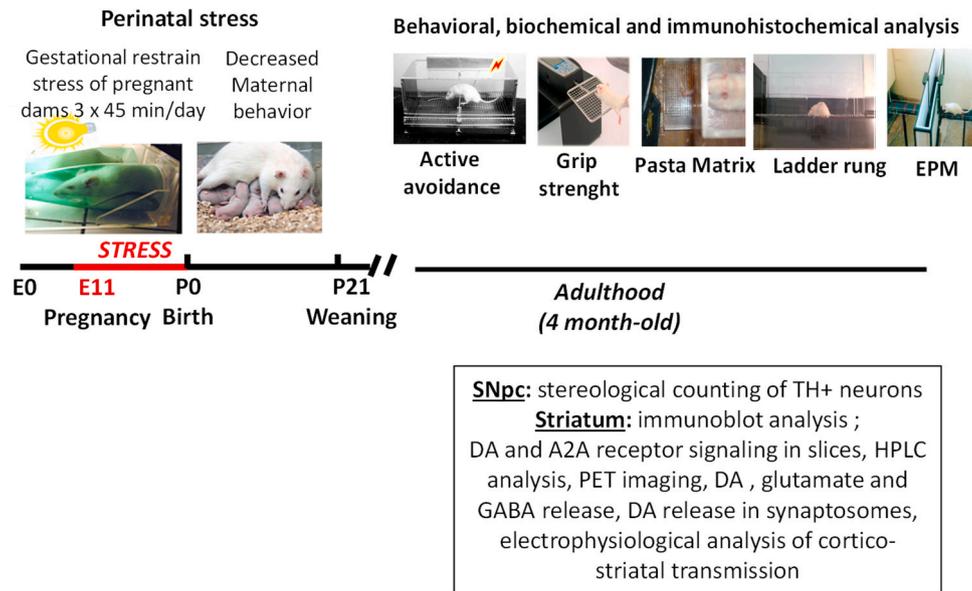
Exp. 2: PRS effects on nigrostriatal dopaminergic transmission and related behavior during lifespan

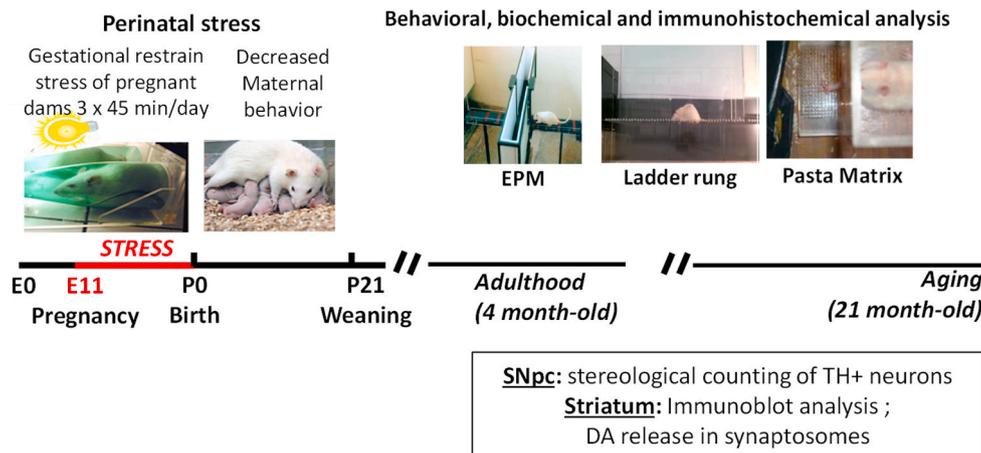**Fig. 1.** Experimental design and timelines of experiments 1 and 2.
Induction of PRS and reduced maternal behavior in the first postpartum week was followed by behavioral and biochemical measurements in the adult (4 months of age) and old (21 months of age) male progeny, as indicated. D_1R, D_2R, and $A_{2A}R = D_1$, D_2, and A_{2A} receptors, respectively; SNpc = *substantia nigra* pars compacta.

2.4.2. Grip strength test

The grip strength of adult and PRS rats was measured using an automated grip strength meter (BiosebLab, Vitrolles, France). The apparatus consisted of a single grip crossbar linked to a single strain gauge connected to a printed circuit chip for a direct digital readout of the measurements. The rats were trained to grasp the grid and subsequently tested for three consecutive days. The rats were held by the tail with their hind limbs over the mesh grid of the meter, and once the forepaws but neither hind-limb were both firmly grasping the grid, the rats were pulled by their tail along the axis of the force sensor until they were unable to retain their grip. Three measurements per trial were averaged for each rat on each day for analysis.

2.4.3. Pasta matrix reaching test

The fine motor skills of adult and aged control and PRS rats were assessed in the pasta matrix-reaching task (adapted from Ballermann et al., 2001). The experimental apparatus consisted of a transparent plexiglass box ($14 \times 35 \times 35$ cm), which housed the animal and included a 4-mm wide vertical slit on one side. A shelf with 230 holes, in which pieces of raw spaghetti (Spaghettini Barilla # 3) were inserted vertically, was placed next to the vertical slit. For one week before the test, the rats were individually housed in single cages and given *spaghetti* pieces in their home cage *ad libitum* in addition to their food pellets. On day 1, the rats were food-deprived at 7:00 p.m. for 24 h and then received the *spaghetti* pieces in their home cage from 7:00 p.m. to 9:00 p.m. the day after (day 2). On day 3, the rats were habituated to the experimental apparatus without *spaghetti* pieces and left undisturbed from 7:00 p.m. to 9:00 p.m. On day 4, the rats were placed in the experimental apparatus containing spaghetti pieces and left undisturbed from 7:00 p.m. to 9:00 p.m. The coordinates and total number of pasta pieces retrieved on day 4 were recorded by observing the pasta shelf at the end of the session. An Excel matrix obtained from the number of retrieved *spaghetti* pieces per box was created to visualize the results, which were plotted as a heat map.

2.4.4. Elevated plus maze

The risk-taking behavior of PRS and control adult and aged progeny was assessed in the elevated plus maze (EPM) (Pellow et al., 1985; Morley-Fletcher et al., 2018). Briefly, the test was performed between 1:00 p.m. and 4:00 p.m., lasted for 5 min, and began by placing the rat in the center of the maze with the head facing a closed arm. For adult animals, we used a standard EPM apparatus with closed and open arms measuring 10×10 cm, while for aged animals, we used a custom-made EPM apparatus as described by Vallée et al. (1999), with closed and open arms measuring 20×20 cm. The luminosity of the closed and open arms was approximately 25 and 50 lux, respectively. Behavior was recorded on-line by a video camera and manually scored by a trained observer blinded to the animals' conditions (PRS or control) using specific software (The Observer®, Noldus, The Netherlands). The duration spent in the open and closed arms was recorded by a video camera and the percentage of time spent in the open arms was calculated.

2.4.5. Ladder rung walking test

The fine motor skills of aged control and PRS rats were assessed using the horizontal ladder rung walking test (Metz and Whishaw, 2002). The apparatus consisted of side walls made of clear Plexiglas and metal rungs (3-mm diameter) that could be inserted to create a floor with a minimum distance of 1 cm between rungs. The sidewalls were 1-m-long and 19-cm-high, as measured from the height of the rungs. The ladder was elevated 30 cm above the ground with a refuge (home cage) at the end. Varying the position of the metal rungs modified the difficulty of the task. A regular pattern of rungs allowed the animals to learn the pattern over several training sessions and to anticipate the rung positions. After the training sessions, an irregular pattern was created to analyze how the rats managed to cross the ladder when the difficulty was increased. The behavior of the rats on the ladder was recorded using two video

cameras: one placed in front of the first half of the ladder at a slight ventral angle and the other in front of the second half of the ladder at a slight ventral angle to precisely analyze the misplacement of the rats' paws. Following the video recording, foot fault scores were analyzed. A score of one was assigned when one paw was misplaced while a score of two was assigned when one paw deeply slipped or missed the rungs. The increase in the percentage of errors between the last training and the test with the irregular pattern was calculated as follows: (error score irregular pattern – error score last training)/error score irregular pattern*100.

2.5. Electrophysiology

Coronal corticostriatal slices were prepared and maintained as described previously (Cacace et al., 2017). Whole-cell patch-clamp recordings were performed as previously described from medium spiny neurons (MSNs) (Bagetta et al., 2012), using infrared differential interference contrast microscopy in the dorsal striatum (Eclipse FN1, Nikon) (Bagetta et al., 2011).

2.6. Induction of long-term depression (LTD) of excitatory transmission in the striatum

After recording evoked excitatory postsynaptic potentials (EPSPs) of stable amplitudes for at least 10 min, LTD was induced using a high-frequency stimulation protocol consisting of three trains of 3 s (20 s interval) at 100 Hz. LTD plots were obtained by averaging the peak amplitudes of the EPSPs every minute. Changes in EPSP amplitude induced by the stimulation protocols were expressed as a percentage of the baseline, the latter representing the normalized EPSP mean amplitude acquired during the stable period (10–15 min) before stimulation.

2.7. Fluorine-18-l-dihydroxyphenylalanine positron emission tomography ($[^{18}F]$-DOPA PET) imaging

The rats were taken to the imaging facility (Univ Lille, Medical Campus) the night before imaging and kept at room temperature with free access to food and water. An IP injection of carbidopa (10 mg/kg, Sigma-Aldrich, Saint-Quentin Fallavier, France) was administered 30–60 min before radiotracer administration.

Each rat was anesthetized with isoflurane (5% for induction and 1.5–2.5% for maintenance at 100% O_2 at a flow rate of 1 L/min) using a nose cone and positioned with the help of a laser alignment device within the scanner such that the center of the field of view was 2 mm caudal to the line between the lateral edges of the eyes. A computed tomography (CT) scan (80 kV and 500 mA) was performed immediately before the rat moved into the PET field of view. An intravenous bolus injection of $[^{18}F]$-DOPA (30 ± 5 MBq; 400–900 μL, IBA-CisBio, Saclay, France) was administered through the caudal vein. PET scanning was initiated at the onset of $[^{18}F]$-DOPA administration. The total scanning time was 55 min. Data from the scanner were formatted into 30 frames, OSEM2D reconstructed, and corrected for scatter and attenuation. The counts detected by the scanner were converted into percentages of injected dose/g using IRW software (Inveon Research Workflow, version 3.0, Siemens), which enables PET-CT co-registration and allows imaging realignment with T2-weighted magnetic resonance images of the rat brain. Regions of interest (ROIs) were manually drawn on the axial and coronal views of the MRI scan and then transferred to the PET images. A background ROI was also drawn outside the brain region. In all cases, the apparent activity in this region reflected the contributions from random coincidence events and scatter, which were found to be very small throughout the study.

2.8. Measurements of catecholamine levels in the striatum

Analysis of DA, 3,4-dihydroxyphenylacetic acid (DOPAC), and

homovanillic acid (HVA) was performed on a high-performance liquid chromatography (HPLC) instrument equipped with an autosampler 507 (Beckman Instruments, Fullerton, CA), a programmable solvent module 126 (Beckman), an analytical C18 reverse-phase column kept at 30 °C (Ultrasphere ODS 5 μm, 80 × pore, 250 × 4.6 mm (Beckman), and a Coulochem II electrochemical detector (ESA, Inc., Chelmsford, MA). The holding potentials were set at +350 and −350 mV for the detection of DA, DOPAC, and HVA. The mobile phase consisted of 80 mM sodium phosphate, 40 mM citric acid, 0.4 mM EDTA, 3 mM 1-heptansulphonic acid, and 12.5% methanol, brought to pH 2.75 with phosphoric acid (run under isocratic conditions at 1 mL/min).

2.9. Microdialysis in freely moving rats

Freely moving control and PRS male rats 5 months of age (350–400 g) were used to assess DA release in the striatum using microdialysis. The rats were implanted with microdialysis intracerebral guides (CMA/12 Guide Cannula, CMA/Microdialysis, Stockholm, Sweden) under isoflurane (5% for induction and 2% for maintenance) anesthesia in a Kopf stereotaxic frame. The site of implantation was the left striatum at the following coordinates: 0.7 mm anterior to the bregma, 2.5 mm lateral to the midline, and 3.5–5.5 mm ventral from the skull surface according to the atlas described by Paxinos and Watson (1998). After surgery, each rat was housed in a cage in a temperature-controlled environment on a 12-h light/dark cycle, with water and food *ad libitum*, and allowed to recover for four days before the experiment. On the evening before the experiment, a concentric vertical microdialysis probe (2-mm-long and 0.24 mm in outer diameter with a cuprophane membrane having a molecular cutoff of 6000 Da, CMA/12 Microdialysis Probe, CMA/Microdialysis) was inserted into the intracerebral guide. After dummy removal, the rat was transferred to a plastic bowl cage with a moving arm (CMA/120 System for Freely-Moving Animals, CMA/Microdialysis) with free access to water and food. The probe was perfused continuously with artificial cerebrospinal fluid containing 150 mM NaCl, 3 mM KCl, 1.7 mM $CaCl_2$, and 0.9 mM $MgCl_2$ at a flow rate of 1.5 μL/min using a microinjection pump (Bioanalytical System Inc., West Lafayette, Indiana, USA). On the following morning, 45 μL (30 min) of consecutive perfusate sample fractions were continuously collected by a fraction collector (CMA/142 Microfraction Collector, CMA/Microdialysis). After four sample fractions, which were used to determine the basal levels of DA, veratridine (100 μM) was perfused for 20 min and sample fractions were collected for the next 2 h. Changes in the perfusion medium were performed using a liquid switch (CMA/111 syringe selector, CMA/Microdialysis) to avoid flow interruption. The analysis of DA was performed as described above.

2.10. Measurements of neurotransmitter release from superfused striatal synaptosomes

Striatal samples were homogenized in 10 vol of 0.32 M sucrose buffered to pH 7.4 with Tris (0.01 M), and synaptosomes were isolated by centrifugation as previously described by Marrocco et al. (2012). The synaptosomal pellet was then resuspended in a medium containing (mM): NaCl, 140; KCl, 3; MgSO4, 1.2; CaCl2, 1.2; NaH2PO4, 1.2; NaHCO3, 5; HEPES, 10 mM; and glucose, 10, at pH 7.2–7.4. Striatal synaptosomes were labeled with [^{3}H]-DA, D-[^{3}H] aspartate or [^{3}H]-gamma-aminobutyric acid (GABA). Labeling of dopaminergic terminals with [^{3}H]-DA was carried out in the presence of ascorbic acid, pargyline, and 6-nitroquipazine and desipramine to avoid labeling of serotonergic or noradrenergic terminals, respectively. The release experiment was performed as described previously by Marrocco et al. (2012).

2.11. Western blot analysis in the striatum

Immunoblot analysis was carried out under standard conditions (Marrocco et al., 2012) using the following primary antibodies: anti-tyrosine hydroxylase (TH H126, Santa Cruz, 1:1000); anti-D1 receptors (Ab20066, Abcam, 1:500), anti-D2 receptors (Ab85367, Abcam, 1:500), anti-DAT (high affinity DA transporter) (ab111468, Abcam, 1:1000); anti-adenosine receptors (sc-13937, Santa Cruz, 1:500), synaptic vesicle-associated proteins: anti-Rab3a (#107111, Synaptic Systems, 1:2000); anti-Munc18 (#116011, Synaptic Systems 1:2000; anti-SNAP 25 (sc-136,267, Santa Cruz 1:5000); anti-SYP (sc-9116 Santa Cruz 1:8000), and anti-syntaxin (sc-13994, Santa Cruz 1:4000). Secondary antibodies directed against rabbit or mouse antibodies (Amersham) were used at 1:7500 dilution. After immunoblotting, digitized images of bands immunoreactive to the target antibodies and actin were acquired (FUSION®) and the area of immunoreactivity corresponding to each band was measured using ImageJ imaging software. The ratios of the targets to actin were then determined and these values were compared to check statistical significance.

2.12. Measurement of cAMP formation in striatal slices

The striatum from adult control and PRS rats were dissected and sliced with a McIlwain tissue chopper (350 × 350 μm). The slices were incubated in Krebs-Henseleit buffer (equilibrated with 95% O_2/5% CO_2, pH 7.4) for 35–45 min at 37 °C under constant oxygenation to allow metabolic recovery. An aliquot (40 μL) of gravity-packed slices was then transferred to polyethylene tubes and incubated for 45 min before the addition of the specific drugs. The slices were incubated with 0.5 mM 3-isobutyl-1-methylxanthine (IBMX) for 15 min and were then challenged with SKF-38393 (10 μM), 2-chloro-adenosine (100 μM and 500 μM, a mixed A_1/A_{2A} receptor agonist), forskolin (10 μM), or quinpirole (10 μM) + forskolin (quinpirole was added 2 min before forskolin). After the addition of the drug, the incubation was continued for 20 min. The reaction was stopped by adding ice-cold 0.4 N $HClO_4$. The samples were then rapidly placed on ice and left at −20 °C overnight. On the day of the experiment, the samples were sonicated for 10–15 s and then added to 2 N K_2CO_3 and centrifuged at low speed. An aliquot of the supernatant was diluted and used for cyclic AMP determination. Cyclic AMP formation was quantified using a commercially available enzyme-linked immunosorbent assay (ELISA) kit (Tema Ricerca, Italy). IBMX, forskolin, SKF-38393, and quinpirole were purchased from Sigma-Aldrich (St. Louis, MO).

2.13. Tyrosine hydroxylase (TH) immunostaining in the substantia nigra

The rats' brains were dissected, fixed in Carnoy solution (ethanol, acetic acid, and chloroform, 6:1:3), and embedded in paraffin. Tissue sections (15 μm) were incubated overnight with mouse monoclonal anti-TH antibodies (1:200, Sigma, Italy, Milano, cat. T1299) and then for 1 h with secondary biotin-coupled anti-mouse antibody (1:200; Vector Laboratories, Burlingame, CA, BA2000). 3,3-Diaminobenzidine tetrachloride (Sigma) was used for detection.

2.14. Stereological cell counting

The number of TH$^+$ cells in the *substantia nigra* was assessed by a stereological technique and optical fractionator using a Zeiss Axio Imager M1 microscope equipped with a motorized stage and focus control system (Zeta axis) and a digital video camera. Image-Pro Plus 6.2 for Windows (Media Cybernetics, Inc., Bethesda, MD) equipped with a macro was used for the analysis of digital images. The macro was obtained from Immagini and Computer (Bareggio, Italy). The analysis was performed on seven 15-μm sections, sampled every 200 μm in a rostrocaudal extension of the *substantia nigra* from the bregma level from 4.80 to −6.30. In each stained section, the area was identified and outlined at 2.5 × magnification. TH + cells were counted at 100 × magnification. For stereological analysis, we used a grid of dissector (counting frame of 50 × 50 μm; grid size 150 × 150 μm). The total

number of TH-immunoreactive neurons per rostrocaudal level was computed using the following formula: $N = \Sigma(n) \times 1/SSF \times 1/ASF \times 1/TSF$, where N is the total number of neurons counted on each dissector, SSF (fraction of sections sampled) is the number of regularly spaced sections used for counts divided by the total number of sections through the *substantia nigra* pars compacta ($= 1/12$); ASF (area sampling frequency) is the dissector area divided by the area between dissectors [= $(2500\ \mu m^2 \times$ dissector number)/region area], and TSF (thickness sampling frequency) is the dissector thickness divided by the section thickness. The total number of TH-immunoreactive neurons in the *substantia nigra* pars compacta was the sum of the total number of TH-immunoreactive neurons per rostrocaudal level.

2.15. Statistical analysis

Behavioral, electrophysiological, and biochemical data were expressed as means ± standard error of the mean and analyzed by parametric analysis of variance (ANOVA) with group as the independent variable (Controls (CONT) *vs.* PRS) and days or treatment as repeated measures (active avoidance and grip strength tests or A_{2A} functionality, respectively). When group × day or treatment interaction was present, post-hoc comparisons were performed using Newman–Keuls tests. The LTD statistical comparisons between different groups over time were analyzed using two-way ANOVA. The level of significance was set at $p < 0.05$.
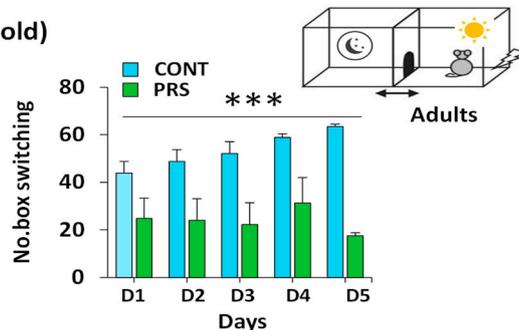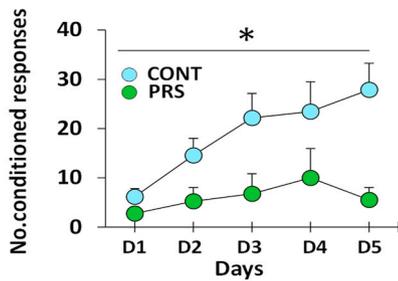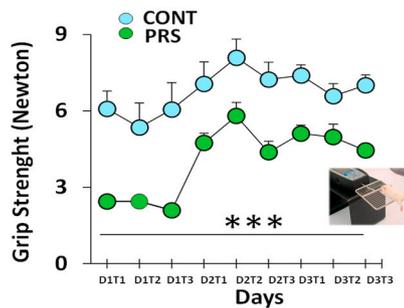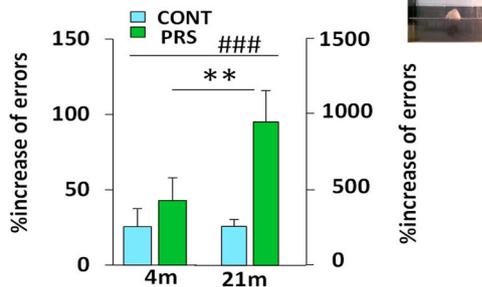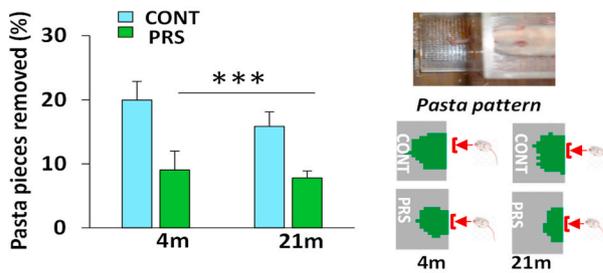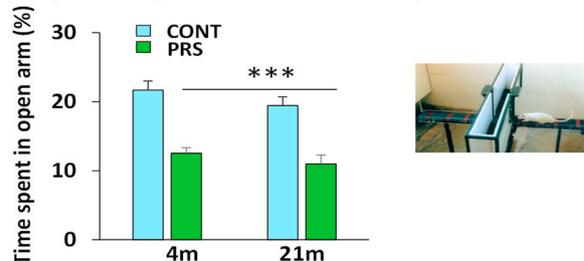

Fig. 2. PRS effects on striatum-dependent behaviors in adulthood and during aging. In the *active avoidance test* (Fig. 2A), PRS reduced the conditioned responses and box switches (n = 6–7 adult rats/group). Four-month-old adult PRS male rats also showed defective striatal motor performance in the *grip strength test* (Fig. 2B) by displaying reduced strength over three consecutive days of training (n = 6 adult rats/group). Aging (21 months) induced defective striatal motor performance only in the *ladder rung-walking test* (n = 6 rats/group, Fig. 2C), in which 21-month-old aged rats showed more errors than did 4-month-old adult rats. While a PRS effect was observed in both age groups, 21-month-old PRS rats showed more errors in the ladder rung-walking test. In the *pasta matrix-reaching test* (Fig. 2D), PRS affected both age groups. PRS rats removed a lower number of pasta pieces than unstressed control rats, with consequently poorer extension of the matrix for PRS rats than for unstressed control rats (n = 6–7 rats/group). In addition, in the *elevated plus maze test* (Fig. 2E), PRS rats of both ages showed lower exploration of the open arm and consequent risk-taking behaviors (n = 7 rats/group). CONT *vs.* PRS *p < 0.05; **p < 0.01; ***p < 0.001; adult *vs.* aged ### = p < 0.001.

3. Results

The experimental design and timelines of experiments 1 and 2 are shown in Fig. 1.

3.1. Effect of PRS on striatum-related behaviors

In the *active avoidance test* (Fig. 2A), the numbers of conditioned responses and box switches were lower among the PRS rats (number of conditioned responses: group effect $F_{(1,11)} = 6.086$, $p = 0.031$; number of box switches: group effect $F_{(1,11)} = 17.691$, $p = 0.001$; n = 6–7 rats/group). Adult (4 months of age) PRS male rats also showed impaired striatal motor performance in the *grip strength test* (Fig. 2B); they exhibited reduced strength over three consecutive days of training (group effect $F_{(1,10)} = 47.682$, $p = 0.000042$; n = 6 rats/group). An interaction between the effect of aging and stress group ($F_{(1,20)} = 9.956$, $p = 0.0049$ n = 6 rats/group) was observed in the *ladder rung walking test* (Fig. 2C). Comparison of adult and aged (21 months of age) rats showed that aging induced defective striatal motor performance in the ladder rung walking test (age effect, $F_{(1,20)} = 28,445$, $p = 0.00004$, n = 6 rats/group). Moreover, we observed a difference between the groups (group

effect $F_{(1,20)} = 11.004$, $p = 0.0034$ n = 6 rats/group); PRS in both adult and aged groups induced more errors during the ladder rung walking test than in unstressed control rats. However, only PRS aged rats made significantly more errors than did the other groups (Newman-Keuls, $p = 0.00015$). PRS affected both age groups in the *pasta matrix reaching test* (Fig. 2D). Compared with unstressed control rats, PRS rats removed a lower number of pasta pieces from the matrix, which was associated with decreased forepaw extension (group effect, $F_{(1,24)} = 15.184$, $p = 0.001$, n = 6–7 rats/group). In addition, in the EPM test (Fig. 2E), PRS rats of both ages showed reduced exploratory activity in the open arm, indicating reduced risk-taking behavior (group effect, $F_{(1,24)} = 54.838$, $p = 0.001$; n = 7 rats/group). The total number of arm entries did not differ between the control and PRS groups for both adult (4 months of age) and aged (21 months of age) rats (interaction group × age, $F_{(1,24)} = 0.04$, $p = 0.8414$). Thus, PRS induced impairment in striatal behavior in both adult and aged rats.

3.2. Effect of PRS on cortico-nigrostriatal synaptic transmission in adulthood (4 months of age)

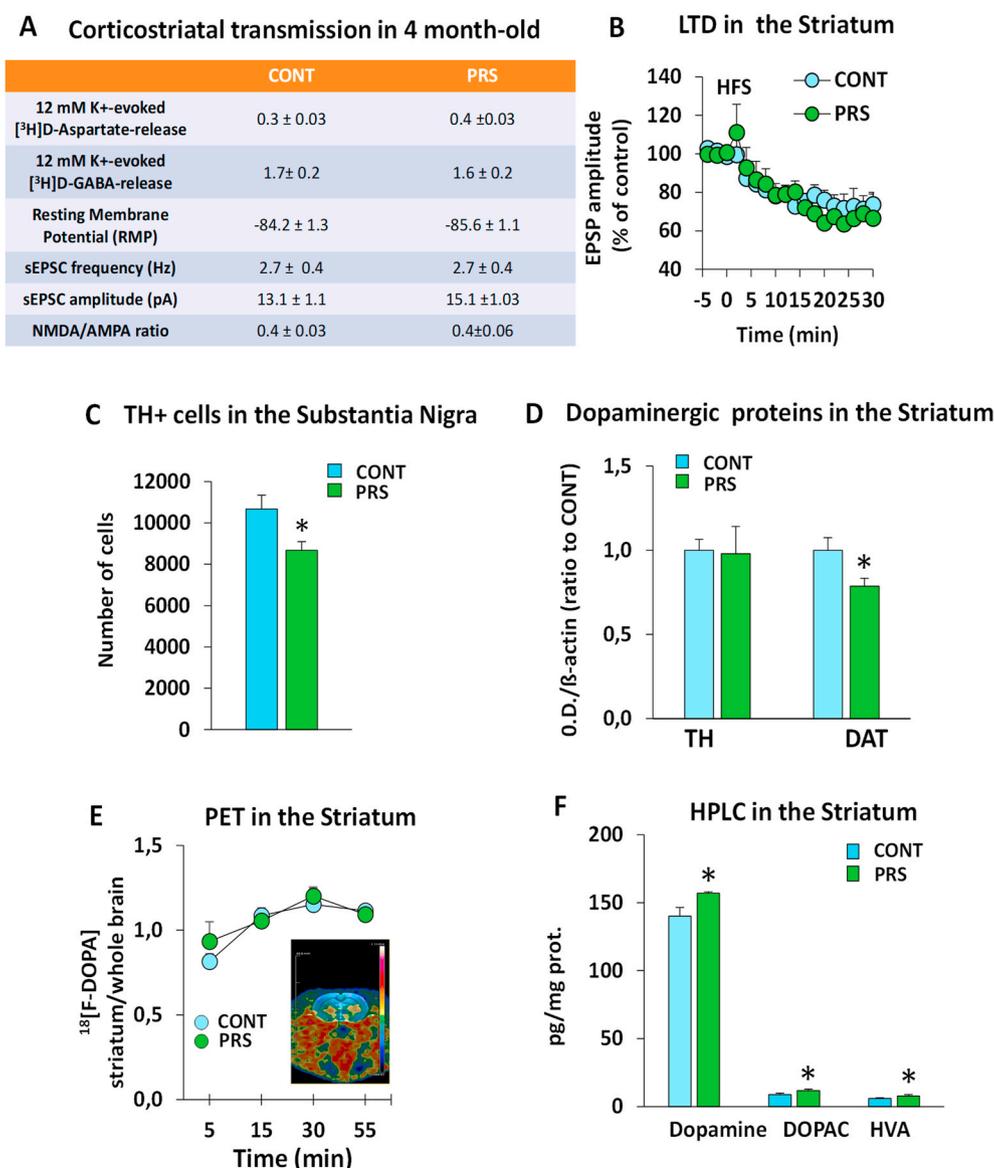As shown in Fig. 3A, the basal and depolarization-evoked release of

A Corticostriatal transmission in 4 month-old

	CONT	PRS
12 mM K+-evoked [³H]D-Aspartate-release	0.3 ± 0.03	0.4 ±0.03
12 mM K+-evoked [³H]D-GABA-release	1.7± 0.2	1.6 ± 0.2
Resting Membrane Potential (RMP)	-84.2 ± 1.3	-85.6 ± 1.1
sEPSC frequency (Hz)	2.7 ± 0.4	2.7 ± 0.4
sEPSC amplitude (pA)	13.1 ± 1.1	15.1 ±1.03
NMDA/AMPA ratio	0.4 ± 0.03	0.4±0.06

B LTD in the Striatum

C TH+ cells in the Substantia Nigra

D Dopaminergic proteins in the Striatum

E PET in the Striatum

F HPLC in the Striatum

Fig. 3. PRS effects on cortico-nigrostriatal synaptic transmission in adulthood (4-month-old rats).

Basal and depolarization-evoked release of glutamate or gamma-aminobutyric acid (GABA) in superfused striatal synaptosomes did not differ between PRS and unstressed control rats (glutamate n = 6 rats/group; GABA release n = 3 rats/group) (Fig. 3A). The striatal projection neurons of PRS rats did not show changes in resting membrane potential (n = 13 rats/group), spontaneous excitatory synaptic transmission (n = 10–15 rats/group), NMDA/AMPA ratio-mediated inward currents (n = 7 Ctrl, 9 PRS), or LTD of the excitatory synaptic transmission in response to high-frequency stimulation of the cortico-striatal pathway (n = 6 rats/group) (Fig. 3B). In the *substantia nigra*, PRS reduced the number of cells expressing the DA synthesizing enzyme tyrosine hydroxylase (TH) (n = 7–8 animals/group, Fig. 3C) but induced no difference in TH protein levels in the striatum (n = 6 adult rats/group, Fig. 3D). In contrast, in the striatum, PRS reduced high-affinity DA transporter (DAT) levels (n = 7 animals/group, Fig. 3D). *In vivo* micro-PET analysis of [¹⁸F]-DOPA uptake in the striatum (n = 4 animals/group) showed no difference between control and PRS rats (Fig. 3E). In contrast, PRS increased the steady-state levels of DA and its metabolites (DOPAC and HVA) in striatal homogenates (n = 10–12 rats/group, Fig. 3F). CONT *vs.* PRS *$p < 0.05$.
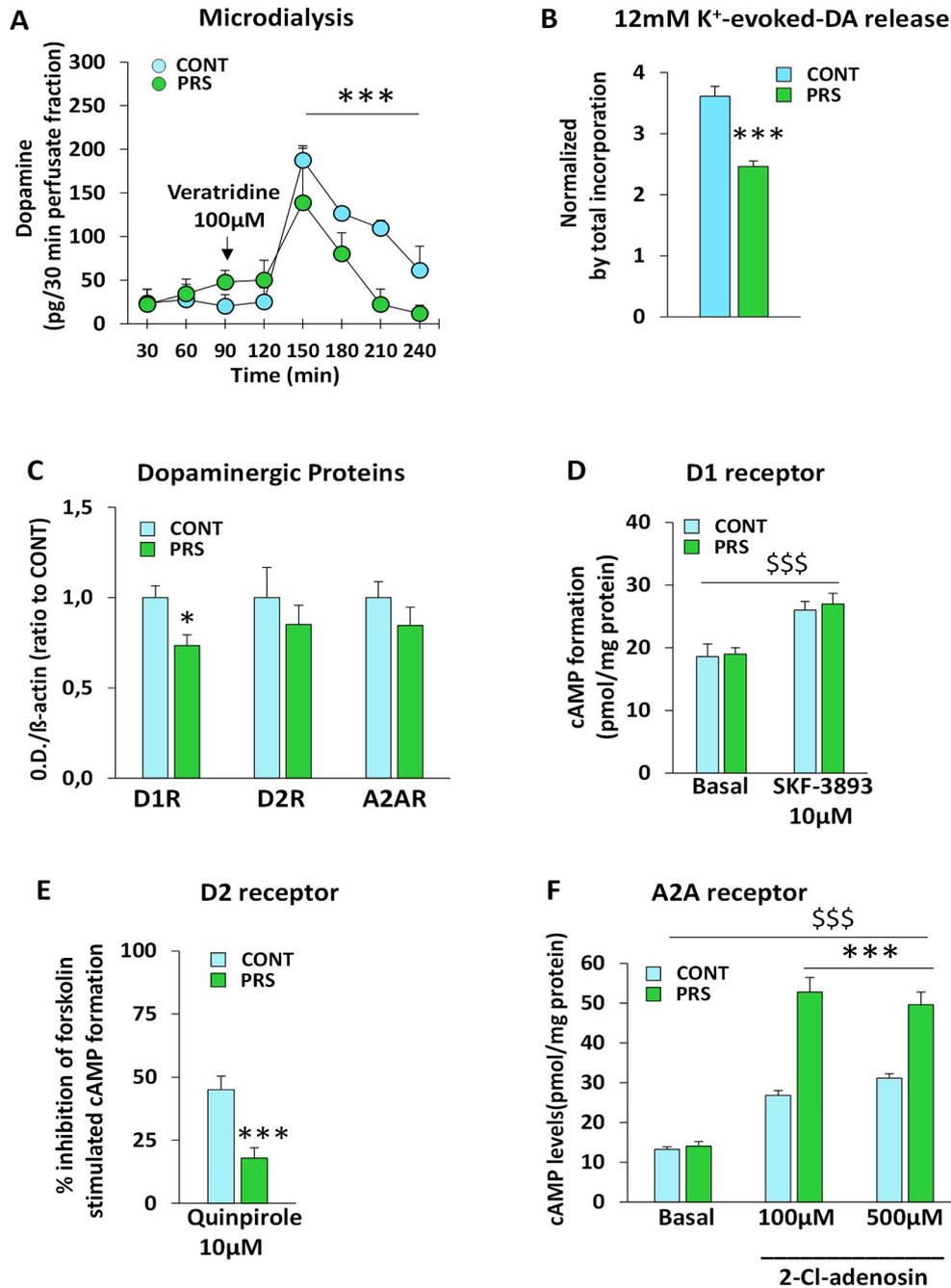
Fig. 4. Effects of PRS on nigrostriatal dopaminergic transmission and indirect and direct pathways in adulthood (4-month-old rats).

PRS reduced DA release in the striatum of adult rats. Microdialysis studies in freely moving rats (Fig. 4A) showed a significant decrease in veratridine-stimulated DA release in the striatum of PRS rats (n = 5 rats/group). A reduction in preloaded [^{3}H]-DA release was also observed in striatal synaptosomes challenged with depolarizing concentrations of K^+ (Fig. 4B) (n = 5 rats/group). Immunoblot analysis (Fig. 4C) revealed that PRS caused a significant reduction in striatal D_1 receptor protein levels, with no changes in the levels of D_2 receptors and A_{2A} adenosine receptors (n = 6 rats/group). Despite the reduction in D_1 receptor protein levels, the ability of the D_1 receptor agonist, SKF-38393, to enhance cAMP formation (n = 6/rats/group) was unchanged in the striatum of PRS rats (n = 6 rats/group) (Fig. 4D). In contrast, PRS reduced D_2 receptor signaling (n = 7–8 rats/group, Fig. 4E) and amplified A_{2A} receptor signaling (n = 4 rats/group, Fig. 4F) in the striatum. CONT *vs.* PRS *p < 0.05; ***p < 0.001; treatment *vs.* basal $$$p < 0.001.

A TH+ cells in Substantia Nigra

B 12mM K+ evoked-DA release in Striatum

C Dopaminergic proteins in Striatum
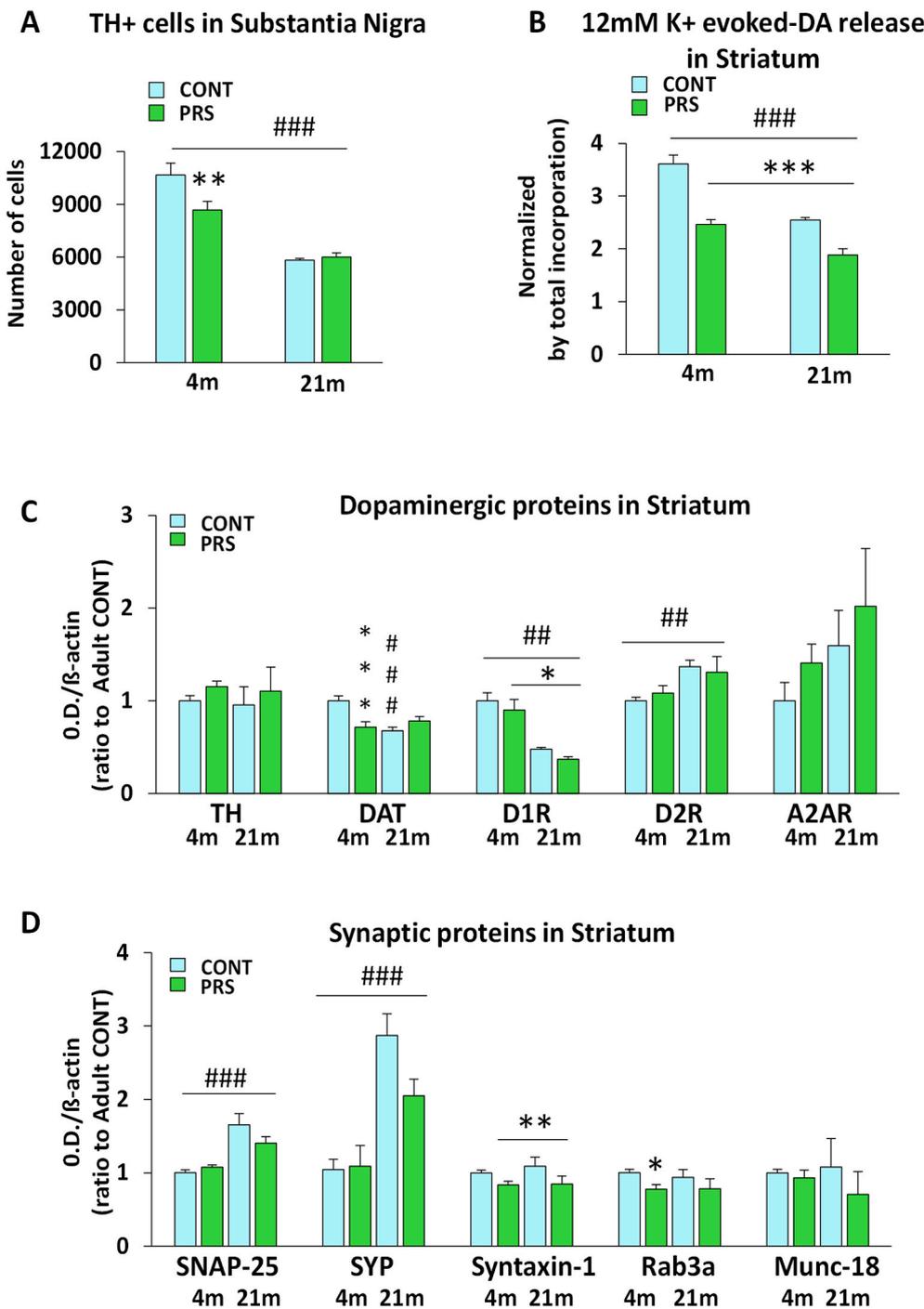
D Synaptic proteins in Striatum

Fig. 5. PRS effects on nigrostriatal dopaminergic transmission throughout the lifespan. Adult PRS rats showed fewer TH-expressing cells than age-matched controls, whereas aged rats in both groups showed fewer TH^{+} cells than did 4-month-old adult rats (Fig. 5A; n = 7–8 rats/group). ^{3}H-DA release evoked by high concentrations of 12 K^{+} in striatal synaptosomes was significantly reduced by PRS in both age groups. Aging (21-month-old rats) reduced DA release in both unstressed and PRS rats (Fig. 5B; n = 5 rats/group). No changes were observed in the striatal levels of TH and $A_{2A}R$ (n = 4–8 rats/group), while an age effect was observed in D_1R in both unstressed and PRS groups, with lower levels than those in adult rats (n = 4–8 rats/group). Aging reduced DAT protein expression only in unstressed rats (n = 4–8 rats/group) and increased D_2R protein levels in both unstressed and PRS rats (n = 4–8 rats/group) (Fig. 5C). PRS reduced syntaxin-1 levels in both ages, but mainly in old rats. PRS also reduced Rab3a levels in both age groups (n = 5–8 rats/group) but mainly in adult rats. In both groups, aging led to higher synaptophysin (SYP) and SNAP-25 levels than those in adults (n = 5–8 rats/group). Neither aging nor PRS did not affected munc-18 protein expression (n = 5–8 rats/group) (Fig. 5D). CONT *vs.* PRS *p < 0.05; **p < 0.01; ***p < 0.001; adult *vs.* aged ###p < 0.001.

glutamate or GABA in superfused striatal synaptosomes did not differ between the PRS and unstressed control groups (group effect: glutamate release, $F_{(1,10)} = 0.024$, $p = 0.87$, n = 6 rats/group; GABA release $F_{(1,4)} = 0.171$, $p = 0.7$, n = 3 rats/group). The striatal projection neurons of the PRS rats did not show changes in resting membrane potential (group effect, $F_{(1,23)} = 0.085$, $p = 0.772$; n = 12–13 rats/group), spontaneous excitatory synaptic transmission (measures in Hz: group effect $F_{(1,22)} = 0.00571$, $p = 0.940$, n = 10–14; measures in pA: group effect $F_{(1,21)} = 1.597$, $p = 0.220$, n = 10–13 rats/group), N-methyl-D-aspartate/α-amino-3-hydroxy-5-methyl-4-isoxazolepropionic acid (NMDA/AMPA) ratio-mediated inward currents (group effect $F_{(1,13)} = 0.00001$, $p = 0.992$, n = 7–8 rats/group), or LTD of excitatory synaptic transmission in response to high-frequency stimulation of the corticostriatal pathway (group × time interaction $F_{(1,18)} = 0.729$, $p = 0.75$; n = 6 rats/group) (Fig. 3B). Thus, no changes in corticostriatal glutamatergic synaptic transmission and plasticity were observed in adult (4 months of age) rats with PRS. Stereological counting in the *substantia nigra* pars compacta showed fewer TH$^+$ cells in PRS rats (Fig. 3C); (group effect: TH + cell counting, $F_{(1,13)} = 6.066$, $p = 0.028$, n = 7–8 animals/group). In the striatum (Fig. 3D), PRS did not induce changes in TH protein levels (*TH immunoblotting*, $F_{(1,2)} = 0.0147$, $p = 0.0906$, n = 6 rats/group), but did reduce DAT levels (group effect: DAT, $F_{(1,12)} = 7.542$, $p = 0.017$; n = 7 rats/group). *In vivo* micro-PET analysis of [^{18}F]-DOPA uptake in the striatum (Fig. 3E) showed no difference between the control and PRS groups (group effect, $F_{(1,6)} = 0.455$, $p = 0.525$, n = 4 rats/group). In contrast, PRS increased the steady-state levels of DA and its metabolites (DOPAC and HVA) in striatal homogenates (Fig. 3F, group effect: DA, $F_{(1,20)} = 6.403$, $p = 0.019$; HVA, $F_{(1,20)} = 6.717$, $p = 0.017$; DOPAC, $F_{(1,20)} = 5.216$, $p = 0.033$; n = 10–12 rats/group).

3.3. Effects of PRS on nigrostriatal dopaminergic transmission and indirect and direct pathways in adulthood (4 months of age)

Microdialysis studies in freely moving rats (Fig. 4A) showed lower veratridine-stimulated DA release in the striatum of PRS rats than in controls (group effect, interval 150–240 min post-veratridine, $F_{(1,8)} = 5.651$, $p = 0.0017$, n = 5 rats/group). Lower preloaded [^{3}H]-DA release was also observed in purified striatal synaptosomes prepared from PRS rats in response to depolarizing concentrations of K+ using an up-down superfusion system that prevented the indirect effects of endogenous molecules on neurotransmitter release (group effect, $F_{(1,8)} = 36.717$, $p = 0.0003$, n = 5 rats/group) (Fig. 4B). Together, the DA neurotransmission measurements suggested that PRS reduced DA release in the striatum of adult (4 months of age) rats. Immunoblot analysis revealed that PRS downregulated striatal D$_1$ receptor protein levels (Fig. 4C), with no changes in D$_2$ and A$_{2A}$ adenosine receptor levels (group effect: D$_1$R, $F_{(1,10)} = 9.088$, $p = 0.013$; D$_2$R $F_{(1,10)} = 0.559$, $p = 0.471$; A$_{2A}$R $F_{(1,10)} = 1.312$, $p = 0.278$; n = 6 rats/group). We extended the analysis of D$_1$, D$_2$, and A$_{2A}$ receptor signaling by measuring cAMP levels in striatal slices from PRS and unstressed controls. Despite the reduction in D$_1$ receptor protein levels, the ability of the D$_1$ receptor agonist SKF-38393 to enhance cAMP formation (treatment effect, $F_{(1,20)} = 30.819$, $p = 0.00002$, n = 6/rats/group) was similar between the striatum of PRS rats and unstressed control rats (group effect: $F_{(1,20)} = 0.591$, $p = 0.450$, n = 6 rats/group) (Fig. 4D). In contrast, PRS reduced D$_2$ (Fig. 4E) and amplified A$_{2A}$ (Fig. 4F) receptor signaling in the striatum. Accordingly, the extent of inhibition of forskolin-stimulated cAMP formation by the D$_2$ receptor agonist, quinpirole, was lower in striatal slices prepared from PRS rats (group effect, $F_{(1,13)} = 15.337$, $p = 0.001$, n = 7–8 rats/group), whereas stimulation of cAMP formation by the A$_{2A}$ receptor agonist, 2-chloroadenosine, a mixed A$_1$/A$_{2A}$ receptor agonist, was amplified (Group × Treatment effect, $F_{(2,18)} = 17.877$, $p = 0.001$, n = 4
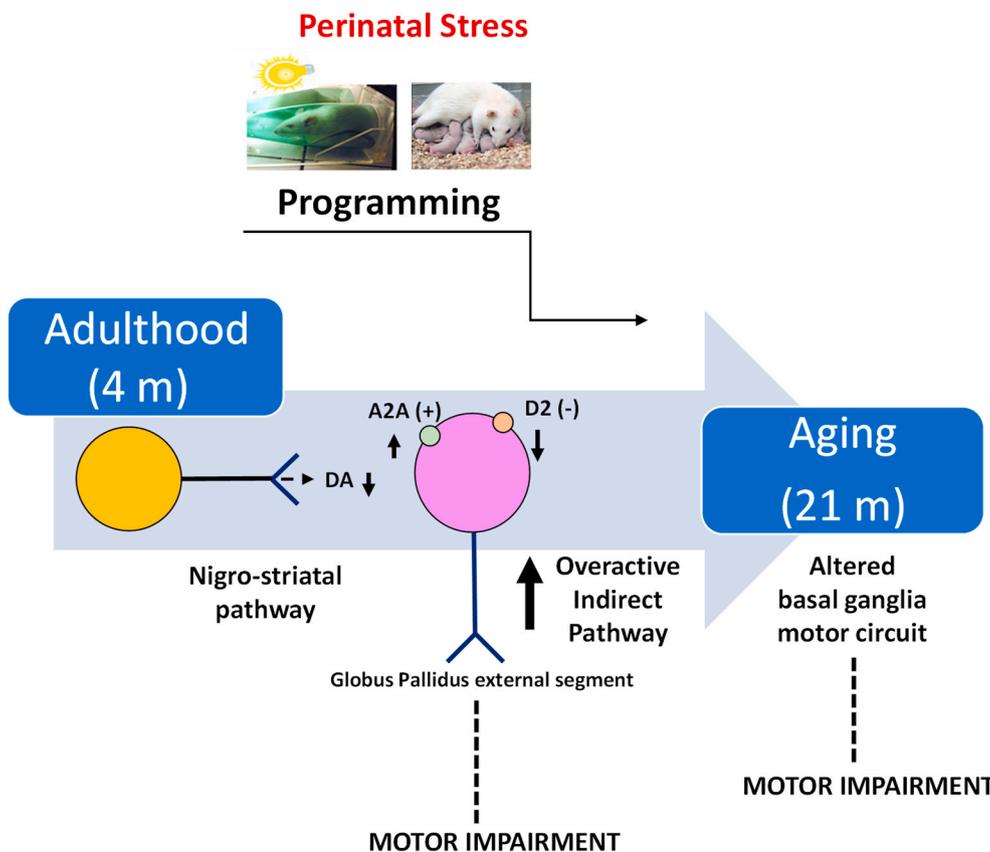

Fig. 6. Modeling dopaminergic transmission in 4-month-old adult and 21-month-old aged PRS rats.

The net effect of nigrostriatal pathway activation is to excite the direct pathway and inhibit the indirect pathway. Four-month-old adult PRS rats showed reduced striatal dopamine release associated with opposite changes in D$_2$ and A$_{2A}$ receptor signaling (which decreased and increased, respectively) in the striatum. D$_2$ and A$_{2A}$ receptors form functional antagonistic heteromers that regulate the activity of striatopallidal neurons of the indirect pathway. The prevalence of A$_{2A}$ over D$_2$ receptor signaling suggests that the indirect pathway is overactive in the striatum of 4-month-old adult PRS rats. This, combined with reduced DA release, reinforces the inhibitory action of the overactive indirect pathway on motor program execution and may account for the lower behavioral performance shown by both 4-month-old adult and 21-month-old aged PRS rats in tests requiring the correct functioning of striatal motor programming.

rats/group). Thus, D_2 and A_{2A} activities were downregulated and upregulated, respectively, in the striatum of adult (4 months of age) PRS rats. The changes in nigrostriatal dopaminergic transmission observed in the adult PRS rats are summarized in the schematic model in Fig. 6.

3.4. Comparison of the effects of PRS on nigrostriatal dopaminergic transmission in adult (4 months of age) and aged (21 months of age) offspring

Absolute numbers of TH^+ cells were lower in both aged PRS and unstressed rat groups than in adult rats (Fig. 5A; age effect, $F_{(1,26)} = 79.535$, $p = 0.0001$; group $\times$ age effect $F_{(1,26)} = 3.490$, $p = 0.073$; *post hoc*: CONT *vs.* PRS in adult $p = 0.0025$, $n = 7$–8 rats/group). ^{3}H-DA release evoked by high concentrations of K^+ (12 mM) in striatal synaptosomes was markedly reduced by PRS in both age groups, while the DA release was similar in adult PRS rats and aged unstressed rats. Aging reduced DA release in both unstressed and PRS rats (Fig. 5B; group effect, $F_{(1,16)} = 63.324$, $p = 0.00000006$; age effect, $F_{(1,16)} = 52.432$, $p = 0.0000002$; $n = 5$ rats/group). We then measured dopaminergic proteins in adult and aged rats (Fig. 5C). No changes were observed in striatal levels of TH and $A_{2A}R$ ($n = 4$–8 rats/group), while an age effect was observed for D_1 receptors in both unstressed and PRS groups, with reduced levels in old rats compared to those in adult rats (D_1R age effect, $F_{(1,21)} = 22.796$, $p = 0.0001$; group effect on reduced levels in PRS compared to controls $F_{(1,21)} = 4.785$, $p = 0.04$; $n = 4$–8 rats/group). In PRS rats, D_1 receptor protein levels were downregulated in both age groups, with a marked effect in adult animals (adult group, CONT *vs.* PRS $p = 0.037$; aged group, CONT *vs.* PRS $p = 0.315$), while the DAT was already low in adult PRS rats. Thus, aging reduced DAT levels only in unstressed rats (DAT group $\times$ age effect $F_{(1,21)} = 17.317$, $p = 0.0004$; $n = 5$–8 rats/group; $p = 0.00008$). Aging also increased D_2 receptor protein levels in both unstressed and PRS groups (D_2R age effect $F_{(1,20)} = 11.576$, $p = 0.002$; $n = 4$–8 rats/group).

The striatal synaptic machinery is shown in Fig. 5D. PRS reduced syntaxin-1 levels in both age groups (syntaxin-1 group effect $F_{(1,21)} = 8.526$, $p = 0.008$), with an added effect in aged (21 months of age) animals (adult group CONT *vs.* PRS $p = 0.07$, aged group CONT *vs.* PRS $p = 0.029$). Rab3a levels were also reduced in PRS rats at both ages (Rab3a group effect $F_{(1,21)} = 5.810$, $p = 0.02$, $n = 5$–8 rats/group); however, a significant group effect was observed only in adult (4 months of age) rats (adult CONT *vs.* PRS adult, $p = 0.044$). Synaptophysin (SYP) levels increased with aging in both unstressed and PRS rats (SYP age effect, $F_{(1,20)} = 21.020$, $p = 0.001$; $n = 5$–8 rats/group). Aging also enhanced SNAP-25 protein levels in both groups (SNAP-25 age effect $F_{(1,21)} = 40.515$, $p = 0.000002$, $n = 5$–8 rats/group). Munc-18 protein levels were not affected by aging or PRS (munc-18: $F_{(1,20)} = 0.530$, $p = 0.474$; $n = 5$–8 rats/group).

4. Discussion

Adult (4-month-old) PRS rats showed poor performance in a battery of behavioral tests that required the correct functioning of striatal motor programming. The results of animal studies and functional imaging studies in humans suggest that the striatum is involved in instrumental conditioning (O'Doherty et al., 2004; Melief et al., 2018) and that an active control over threat in the active avoidance test engages the striatum (Boeke et al., 2017). The grip strength test in rats, which measures muscular tension and rigidity, is also dependent on the correct functioning of the nigrostriatal system. In the grip strength test, lesions of the nigrostriatal system enhance muscular force (Dunnett et al., 1998; Ma et al., 2014), which may reflect a rat homolog of rigidity, which is a hallmark feature of DA loss in PD (Dunnett et al., 1998). These PRS-induced changes persisted in the 21-month-old (aged) rats. This finding is highly relevant from a translational standpoint as age is an established risk factor for mobility decline and PD. In both adult and aged PRS rats, we observed impaired behavioral performance in the

pasta matrix-reaching test, which measures reaching distance, direction, and dexterity in rats, and in the horizontal ladder rung walking test, a task that allows the evaluation of fore- and hindlimb stepping, placing, and coordination. Lesions in the nigrostriatal system also affect these behavioral tests (Metz and Whishaw, 2002; Ballermann et al., 2001). Adult and aged PRS rats showed reduced risk-taking behavior in the open arm of the EPM. Although the EPM is not generally considered a striatum-dependent test, dopamine receptor agonists enhance the risk-taking behaviors measured in this test (Drui et al., 2014). In the pasta matrix test and the EPM, adult and aged rats behaved similarly, whereas the aged rats showed poorer performance in the ladder-rung walking test, in which the deteriorating effect of PRS became significant only during aging (21 months), with only a trend observed in adult (4-month-old) rats. Finally, we observed no difference in the total arm entries between control and PRS rats in the EPM in both age groups. This finding suggests that the observed effects occurred specifically due to the impairment of striatal behavior rather than locomotor impairment.

Neurochemical changes found in the striatum of adult PRS rats are suggestive of impaired nigrostriatal dopaminergic transmission associated with increased activity of the indirect pathway. The most consistent change found in both 4- and 21-month-old PRS rats was reduced striatal DA release. In the 4-month-old (adult) PRS rats, the dopaminergic changes could not be ascribed to a nonspecific impairment in the release machinery because levels of synaptic vesicle-associated proteins (except Rab3a) and glutamate and GABA release were unchanged. In addition, in the *substantia nigra*, PRS and aging reduced the number of cells expressing TH. PRS also reduced the striatal levels of DAT. Collectively, these findings may at least partially explain the reduction in DA release in the striatum of both adult and aged PRS rats. Surprisingly, PRS induced no changes in striatal TH protein levels in rats but increased striatal levels of DA and its metabolites. This could reflect a compensatory effect in response to high corticosterone levels induced by PRS (Maccari et al., 1995), as corticosterone enhances catecholamine and TH levels (Busceti et al., 2019). Moreover, early-life stress has been previously reported to increase corticosterone levels in the striatum (Mpofana et al., 2016). A small increase in the density of [^{3}H]-nemonapride-labeled D_2 receptors was reported in the medial caudate/putamen of PRS rats (Adrover et al., 2007). In contrast, we found a reduction in D_1 and no changes in D_2 receptor protein levels in the striatum of 4-month-old adult PRS rats. The reduction in D_1 receptor expression was consistent with the poor motor performance of PRS rats because selective D_1 receptor agonists display anti-parkinsonian activity (Asin et al., 1997; Martini et al., 2019). Interestingly, we observed opposite changes in D_2 and A_{2A} receptor signaling (which decreased and increased, respectively) in the striatum of 4-month-old adult PRS rats. D_2 and A_{2A} receptors form functional antagonistic heteromers that regulate the activity of striatopallidal neurons of the indirect pathway (Ferrè et al., 2008; Calabresi et al., 2013). Therefore, A_{2A} receptor antagonists are under clinical development for the treatment of PD (Armantero et al., 2011). The prevalence of A_{2A} over D_2 receptor signaling in the striatum may also contribute to the impairment in striatum-dependent motor performance in PRS rats. A_{2A} receptors are particularly sensitive to stress-related mechanisms because the overexpression of A_{2A} receptors induces age-like hypothalamic-pituitary-adrenal (HPA) axis dysfunction by changing hippocampal glucocorticoid receptor activity (Batalha et al., 2016), while A_{2A} receptor blockade corrects behavioral, electrophysiological, and morphological abnormalities and restores HPA axis activity in rats subjected to maternal separation (Batalha et al., 2013). As shown in Fig. 6, this suggests that the hyperactivity of the indirect pathway—including a prevalence of A_{2A} over D_2 receptor signaling—combined with reduced DA release and D_2 receptor activity, as observed in 4-month-old adult PRS rats, may be associated with the poorer performance of these animals in the behavioral tests and an increased risk for persistent and long-lasting behavioral disorders during aging (21-month-old rats).

We were surprised that no changes in striatal glutamatergic

transmission and glutamate-dependent synaptic plasticity were found in PRS rats because this was not consistent with previous reports, in which different paradigms of PRS were used. For example, a reduction in the transcript encoding the EAAT2 (GLT-1) glial glutamate transporter was found in the striatum of juvenile (P30) offspring of dams exposed to late but not mid stress during pregnancy (Zhang et al., 2013), and a reduction in the short isoform of the Homer protein (Homer-1a) was found in P21 offspring of dams exposed to stress in the last week of pregnancy (Ary et al., 2007). In addition, PRS delivered during the last week of pregnancy caused astroglial hypertrophy in the striatal matrix (Barros et al., 2006), thereby altering the glial-dependent regulation of glutamate homeostasis. Others and we have consistently found that early-life stress induces robust changes in glutamatergic transmission and activity-dependent synaptic plasticity in the hippocampus and prefrontal cortex (Son et al., 2006; Marrocco et al., 2012; Wang et al., 2016; Morley-Fletcher et al., 2018), two brain regions that are interconnected with striatum and could indirectly affect striatal glutamatergic transmission. The lack of apparent changes in striatal glutamatergic transmission under our experimental conditions might reflect the development of compensation mechanisms aimed at preserving striatal function, bearing in mind that striatal LTD is both dopamine- and glutamate-dependent (Mathur et al., 2011).

Aging also impairs nigrostriatal development. In the *substantia nigra*, reduced numbers of TH-expressing cells were observed in aged rats. Aging (21 months) reduced DAT in the striatum of rats in both groups of PRS rats. We also observed a reduced effect of aging on D_1 receptors, while aging increased D_2 receptor proteins in both unstressed and PRS groups. The increased D_2 receptor protein levels during aging could represent a compensatory mechanism to mitigate age-dependent impairment in striatal motor programming. Accumulating evidence highlights the role of synaptic vesicle-associated proteins in neurodevelopmental and neurodegenerative disorders. The functionality of the SNARE protein interactome is considered a major determinant of the cognitive reserve during aging (Ramos-Miguel et al., 2018). Aged rats showed increased striatal levels of synaptophysin and SNAP-25. SNAP-25 levels are elevated in the cerebrospinal fluid of patients with neurodegenerative disorders or mild cognitive impairment (Brinkmalm et al., 2014), suggesting that SNAP-25 is a candidate biomarker for synapse degeneration. SNAP-25 co-localizes with D_1 receptors in cultured dopaminergic cells, and genetic deletion of SNAP-25 downregulates D_1 receptors in these cells (Yang et al., 2019). In the present study, PRS reduced Rab3a protein levels in 4-month-old adult rats (with a trend in aged rats) and syntaxin levels in both 4-month-old adult and 21-month-old aged rats. This finding suggested that PRS and aging predisposed the rats to long-term dysfunction of the release machinery in the striatum.

In conclusion, the results of this study showed that PRS in rats caused life-long abnormalities in nigrostriatal dopaminergic transmission and reduced the performance of striatum-dependent motor tasks. In adult rats 4 months of age, hyperactivity of the indirect pathway caused by reduced DA release and opposite alterations in D_2 and A_{2A} receptor signaling may lie at the core of these basal ganglia motor dysfunctions. We suggest that PRS accelerates striatal aging by altering the developmental trajectory of the basal ganglia motor circuit, which may lower the age-dependent threshold for motor dysfunction. Dallé and Mabandla (2018) demonstrated that early-life stress can induce depression and that patients with depression are at risk of developing PD later in life. Together, these findings shed light on the nature of the motor developmental programming induced by early-life stress and indicate that early-life stress is a risk factor for motor disorders in older individuals. This raises the possibility that understanding early-life stress, which is poorly investigated, could contribute to an increased understanding of the programing of human motor diseases in adulthood and aging.

Credit author statement

SM and FN conceived and designed the study; JM, RV, DB, LDM, AT, HB, GVC, VG, BP, PC, LR, FC, FB, AP, VB, GB, SMF, FN, and SM acquired and analyzed the data; JM, RV, HB, GB, BP, PC, SMF, FN, and SM drafted significant portions of the manuscript or figures.

Author contribution

J Marrocco, Formal analysis, Data curation, acquired and analyzed the data; drafted significant portions of the manuscript or figures. R Verhaeghe, Formal analysis, Data curation, acquired and analyzed the data; drafted significant portions of the manuscript or figures. D Bucci, Formal analysis, Data curation, acquired and analyzed the data; L Di Menna, Formal analysis, Data curation, acquired and analyzed the data; A Traficante, Formal analysis, Data curation, acquired and analyzed the data; H Bouwalerh, Formal analysis, Data curation, acquired and analyzed the data; drafted significant portions of the manuscript or figures. G Van Camp, Formal analysis, Data curation, acquired and analyzed the data; V Ghiglieri, Formal analysis, Data curation, acquired and analyzed the data; B Piccone, Formal analysis, Data curation, acquired and analyzed the data; drafted significant portions of the manuscript or figures. P Calabresi, Formal analysis, Data curation, acquired and analyzed the data; drafted significant portions of the manuscript or figures. L Ravasi, Formal analysis, Data curation, acquired and analyzed the data; F Cisani, Formal analysis, Data curation, acquired and analyzed the data; F Bagheri, Formal analysis, Data curation, acquired and analyzed the data; A Pittaluga, Formal analysis, Data curation, acquired and analyzed the data; V Bruno, Formal analysis, Data curation, acquired and analyzed the data; G Battaglia, Formal analysis, Data curation, acquired and analyzed the data; drafted significant portions of the manuscript or figures. S Morley-Fletcher, Formal analysis, Data curation, Writing - original draft, acquired and analyzed the data; drafted significant portions of the manuscript or figures. F Nicoletti, Formal analysis, Data curation, Writing - original draft, conceived and designed the study; acquired and analyzed the data; drafted significant portions of the manuscript or figures. S Maccari: Formal analysis, Data curation, Writing - original draft, conceived and designed the study; acquired and analyzed the data; drafted significant portions of the manuscript or figures.

Declaration of competing interest

Any relevant conflicts of interest for each author.

References

Adrover, E., Berger, M.A., Pérez, A.A., Tarazi, F.I., Antonelli, M.C., 2007. Effects of prenatal stress on dopamine D2 receptor asymmetry in rat brain. Synapse 61, 459–462. https://doi.org/10.1002/syn.20389.

Alonso, S.J., Navarro, E., Santana, C., Rodriguez, M., 1997. Motor lateralization, behavioral despair and dopaminergic brain asymmetry after prenatal stress. Pharmacol. Biochem. Behav. 58, 443–448. https://doi.org/10.1016/s0091-3057(97)00009-9.

Armentero, M.T., Pinna, A., Ferré, S., Lanciego, J.L., Müller, C.E., Franco, R., 2011. Past, present and future of A(2A) adenosine receptor antagonists in the therapy of Parkinson's disease. Pharmacol. Ther. 132, 280–299. https://doi.org/10.1016/j.pharmthera.2011.07.004.

Ary, A.W., Aguilar, V.R., Szumlinski, K.K., Kippin, T.E., 2007. Prenatal stress alters limbo-corticostriatal Homer protein expression. Synapse (New York, N.Y.) 61 (11), 938–941. https://doi.org/10.1002/syn.20439.

Asin, K.E., Domino, E.F., Nikkel, A., Shiosaki, K., 1997. The selective dopamine D1 receptor agonist A-86929 maintains efficacy with repeated treatment in rodent and primate models of Parkinson's disease. J. Pharmacol. Exp. Therapeut. 281 (1), 454–459.

Bagetta, V., Picconi, B., Marinucci, S., Sgobio, C., Pendolino, V., Ghiglieri, V., Fusco, F.R., Giampà, C., Calabresi, P., 2011. Dopamine-dependent long-term depression is expressed in striatal spiny neurons of both direct and indirect pathways: implications for Parkinson's disease. J. Neurosci. 31, 12513–12522. https://doi.org/10.1523/jneurosci.2236-11.2011.

Bagetta, V., Sgobio, C., Pendolino, V., Del Papa, G., Tozzi, A., Ghiglieri, V., Giampà, C., Zianni, E., Gardoni, F., Calabresi, P., Picconi, B., 2012. Rebalance of striatal NMDA/AMPA receptor ratio underlies the reduced emergence of dyskinesia during D2-like dopamine agonist treatment in experimental Parkinson's disease. J. Neurosci. 32, 17921–17931. https://doi.org/10.1523/jneurosci.2664-12.2012.

Ballermann, M., Metz, G.A., McKenna, J.E., Klassen, F., Whishaw, I.Q., 2001. The pasta matrix reaching task: a simple test for measuring skilled reaching distance, direction, and dexterity in rats. J. Neurosci. Methods 106, 39–45. https://doi.org/10.1016/s0165-0270(01)00326-0.

Barlow, S.M., Knight, A.F., Sullivan, F.M., 1978. Delay in postnatal growth and development of offspring produced by maternal restraint stress during pregnancy in the rat. Teratology 18, 211–218. https://doi.org/10.1002/tera.1420180206.

Barros, V.G., Duhalde-Vega, M., Caltana, L., Brusco, A., Antonelli, M.C., 2006. Astrocyte-neuron vulnerability to prenatal stress in the adult rat brain. J. Neurosci. Res 83 (5), 787–800. https://doi.org/10.1002/jnr.20758.

Batalha, V.L., Ferreira, D.G., Coelho, J.E., Valadas, J.S., Gomes, R., Temido-Ferreira, M., Shmidt, T., Baqi, Y., Buée, L., Müller, C.E., Hamdane, M., Outeiro, T.F., Bader, M., Meijsing, S.H., Sadri-Vakili, G., Blum, D., Lopes, L.V., 2016. The caffeine-binding adenosine A2A receptor induces age-like HPA-axis dysfunction by targeting glucocorticoid receptor function. Sci. Rep. 6, 31493. https://doi.org/10.1038/srep31493.

Batalha, V.L., Pego, J.M., Fontinha, B.M., Costenla, A.R., Valadas, J.S., Baqi, Y., Radjainia, H., Müller, C.E., Sebastião, A.M., Lopes, L.V., 2013. Adenosine A(2A) receptor blockade reverts hippocampal stress-induced deficits and restores corticosterone circadian oscillation. Mol. Psychiatr. 18 (3), 320–331. https://doi.org/10.1038/mp.2012.8.

Boeke, E.A., Moscarello, J.M., LeDoux, J.E., Phelps, E.A., Hartley, C.A., 2017. Active avoidance: neural mechanisms and attenuation of pavlovian conditioned responding. J. Neurosci. 37, 4808–4818. https://doi.org/10.1523/jneurosci.3261-16.2017.

Brinkmalm, A., Brinkmalm, G., Honer, W.G., Frölich, L., Hausner, L., Minthon, L., Hansson, O., Wallin, A., Zetterberg, H., Blennow, K., Ohrfelt, A., 2014. SNAP-25 is a promising novel cerebrospinal fluid biomarker for synapse degeneration in Alzheimer's disease. Mol. Neurodegener. 9, 53. https://doi.org/10.1186/1750-1326-9-53.

Busceti, C.L., Ferese, R., Bucci, D., Ryskalin, L., Gambardella, S., Madonna, M., Nicoletti, F., Fornai, F., 2019. Corticosterone upregulates gene and protein expression of catecholamine markers in organotypic brainstem cultures. Int. J. Mol. Sci. 20 (12) https://doi.org/10.3390/ijms20122901 pii: E2901.

Cacace, F., Mineo, D., Viscomi, M.T., Latagliata, E.C., Mancini, M., Sasso, V., Vannelli, A., Pascucci, T., Pendolino, V., Marcello, E., Pelucchi, S., Puglisi-Allegra, S., Molinari, M., Picconi, B., Calabresi, P., Ghiglieri, V., 2017. Intermittent theta-burst stimulation rescues dopamine-dependent corticostriatal synaptic plasticity and motor behavior in experimental parkinsonism: possible role of glial activity. Mov. Disord. 32, 1035–1046. https://doi.org/10.1002/mds.26982.

Calabresi, P., Di Filippo, M., Gallina, A., Wang, Y., Stankowski, J.N., Picconi, B., Dawson, V.L., Dawson, T.M., 2013. New synaptic and molecular targets for neuroprotection in Parkinson's disease. Mov. Disord. 28, 51–60. https://doi.org/10.1002/mds.25096.

Calabresi, P., Picconi, B., Tozzi, A., Ghiglieri, V., Di Filippo, M., 2014. Direct and indirect pathways of basal ganglia: a critical reappraisal. Nat. Neurosci. 17, 1022–1030. https://doi.org/10.1038/nn.3743.

Cenci, M.A., Ohlin, K.E., Rylander, D., 2009. Plastic effects of L-DOPA treatment in the basal ganglia and their relevance to the development of dyskinesia. Park. Relat. Disord. https://doi.org/10.1016/s1353-8020(09)70782-5. S59-63.

Clark, P.J., Ghasem, P.R., Mika, A., Day, H.E., Herrera, J.J., Greenwood, B.N., Fleshner, M., 2014. Wheel running alters patterns of uncontrollable stress-induced cfos mRNA expression in rat dorsal striatum direct and indirect pathways: a possible role for plasticity in adenosine receptors. Behav. Brain Res. 272, 252–263. https://doi.org/10.1016/j.bbr.2014.07.006.

Conn, P.J., Battaglia, G., Marino, M.J., Nicoletti, F., 2005. Metabotropic glutamate receptors in the basal ganglia motor circuit. Nat. Rev. Neurosci. 6, 787–798. https://doi.org/10.1038/nrn1763.

Dallé, E., Mabandla, M.V., 2018. Early life stress, depression and Parkinson's disease: a new approach. Mol. Brain 11 (1), 18. https://doi.org/10.1186/s13041-018-0356-9 (submitted for publication).

Deminière, J.M., Piazza, P.V., Guegan, G., Abrous, N., Maccari, S., Le Moal, M., Simon, H., 1992. Increased locomotor response to novelty and propensity to intravenous amphetamine self-administration in adult offspring of stressed mothers. Brain Res. 586, 135–139. https://doi.org/10.1016/0006-8993(92)91383-.

Drui, G., Carnicella, S., Carcenac, C., Favier, M., Bertrand, A., Boulet, S., Savasta, M., 2014. Loss of dopaminergic nigrostriatal neurons accounts for the motivational and affective deficits in Parkinson's disease. Mol. Psychiatr. 19, 358–367. https://doi.org/10.1038/mp.2013.3.

Dunnett, S.B., Torres, E.M., Annett, L.E., 1998. A lateralised grip strength test to evaluate unilateral nigrostriatal lesions in rats. Neurosci. Lett. 246, 1–4. https://doi.org/10.1016/s0304-3940(98)00194-3.

Ferré, S., Quiroz, C., Woods, A.S., Cunha, R., Popoli, P., Ciruela, F., Lluis, C., Franco, R., Azdad, K., Schiffmann, S.N., 2008. An update on adenosine A2A-dopamine D2 receptor interactions: implications for the function of G protein-coupled receptors. Curr. Pharmaceut. Des. 14, 1468–1474. https://doi.org/10.2174/138161208784480108.

Fride, E., Weinstock, M., 1988. Prenatal stress increases anxiety related behavior and alters cerebral lateralization of dopamine activity. Life Sci. 42, 1059–1065. https://doi.org/10.1016/0024-3205(88)90561-9.

Gatta, E., Mairesse, J., Deruyter, L., Marrocco, J., Van Camp, G., Bouwalerh, H., Lo Guidice, J.M., Morley-Fletcher, S., Nicoletti, F., Maccari, S., 2018. Reduced maternal behavior caused by gestational stress is predictive of life span changes in risk-taking behavior and gene expression due to altering of the stress/anti-stress balance. Neurotoxicology 66, 138–149. https://doi.org/10.1016/j.neuro.2018.04.005.

Ida, Y., Tanaka, M., Kohno, Y., Tsuda, A., Hoaki, Y., Nakagawa, R., Iimori, K., Nagasaki, N., 1982. Effects of age and stress on dopamine levels in basal ganglia of rats. Kurume Med. J. 29, 97–99. https://doi.org/10.2739/kurumemedj.29.97.

Lauretti, E., Di Meco, A., Merali, S., Praticò, D., 2016. Chronic behavioral stress exaggerates motor deficit and neuroinflammation in the MPTP mouse model of Parkinson's disease. Transl. Psychiatry 733, 1–6. https://doi.org/10.1038/tp.2016.1.

Ma, Y., Zhan, M., OuYang, L., Li, Y., Chen, S., Wu, J., Chen, J., Luo, C., Lei, W., 2014. The effects of unilateral 6-OHDA lesion in medial forebrain bundle on the motor, cognitive dysfunctions and vulnerability of different striatal interneuron types in rats. Behav. Brain Res. 266, 37–45. https://doi.org/10.1016/j.bbr.2014.02.039.

Maccari, S., Krugers, H.J., Morley-Fletcher, S., Szyf, M., Brunton, P.J., 2014. The consequences of early-life adversity: neurobiological, behavioural and epigenetic adaptations. J. Neuroendocrinol. 26, 707–723. https://doi.org/10.1111/jne.12175.

Maccari, S., Piazza, P.V., Kabbaj, M., Barbazanges, A., Simon, H., Le Moal, M., 1995. Adoption reverses the long-term impairment in glucocorticoid feedback induced by prenatal stress. J. Neurosci. 15, 110–116. https://doi.org/10.1523/jneurosci.15-01-00110.1995.

Maccari, S., Polese, D., Reynaert, M.L., Amici, T., Morley-Fletcher, S., Fagioli, F., 2017. Early-life experiences and the development of adult diseases with a focus on mental illness: the Human Birth Theory. Neuroscience 342, 232–251. https://doi.org/10.1016/j.neuroscience.2016.05.042.

Marrocco, J., Mairesse, J., Bucci, D., Lionetto, L., Battaglia, G., Consolazione, M., Ravasi, L., Simmaco, M., Morley-Fletcher, S., Maccari, S., Nicoletti, F., 2013. Early life stress causes refractoriness to haloperidol-induced catalepsy. Mol. Pharmacol. 84, 244–251. https://doi.org/10.1124/mol.113.085530.

Marrocco, J., Mairesse, J., Ngomba, R.T., Silletti, V., Van Camp, G., Bouwalerh, H., Summa, M., Pittaluga, A., Nicoletti, F., Maccari, S., Morley-Fletcher, S., 2012. Anxiety-like behavior of prenatally stressed rats is associated with a selective reduction of glutamate release in the ventral hippocampus. J. Neurosci. 32, 17143–17154. https://doi.org/10.1523/jneurosci.1040-12.2012.

Martini, M.L., Ray, C., Yu, X., Liu, J., Pogorelov, V.M., Wetsel, W.C., Huang, X.P., McCorvy, J.D., Caron, M.G., Jin, J., 2019. Designing functionally selective noncatechol dopamine D(1) receptor agonists with potent in vivo antiparkinsonian activity. ACS Chem. Neurosci. 10 (9), 4160–4182. https://doi.org/10.1021/acschemneuro.9b00410.

Mathur, B.N., Capik, N.A., Alvarez, V.A., Lovinger, D.M., 2011. Serotonin induces long-term depression at corticostriatal synapses. J. Neurosci. : the official journal of the Society for Neuroscience 31 (20), 7402–7411. https://doi.org/10.1523/JNEUROSCI.6250-10.2011.

Melief, E.J., McKinley, J.W., Lam, J.Y., Whiteley, N.M., Gibson, A.W., Neumaier, J.F., Henschen, C.W., Palmiter, R.D., Bamford, N.S., Darvas, M., 2018. Loss of glutamate signaling from the thalamus to dorsal striatum impairs motor function and slows the execution of learned behaviors. NPJ Parkinsons Dis 4, 23. https://doi.org/10.1038/s41531-018-0060-6.

Metz, G.A., Whishaw, I.Q., 2002. Cortical and subcortical lesions impair skilled walking in the ladder rung walking test: a new task to evaluate fore- and hindlimb stepping, placing, and co-ordination. J. Neurosci. Methods 115, 169–179. https://doi.org/10.1016/s0165-0270(02)00012-2.

Morley-Fletcher, S., Zuena, A.R., Mairesse, J., Gatta, E., Van Camp, G., Bouwalerh, H., Riozzi, B., Battaglia, G., Pittaluga, A., Olivero, G., Mocaer, E., Bretin, S., Nicoletti, F., Maccari, S., 2018. The reduction in glutamate release is predictive of cognitive and emotional alterations that are corrected by the positive modulator of AMPA receptors S 47445 in perinatal stressed rats. Neuropharmacology 135, 284–296. https://doi.org/10.1016/j.neuropharm.2018.03.018.

Mpofana, T., Daniels, W.M., Mabandla, M.V., 2016. Exposure to early life stress results in epigenetic changes in neurotrophic factor gene expression in a parkinsonian rat model. Parkinsons Dis 6438783. https://doi.org/10.1155/2016/6438783.

O'Doherty, J., Dayan, P., Schultz, J., Deichmann, R., Friston, K., Dolan, R.J., 2004. Dissociable roles of ventral and dorsal striatum in instrumental conditioning. Science 304, 452–454. https://doi.org/10.1126/science.1094285.

Paxinos, G., Watson, C., 1998. The Rat Brain in Stereotaxic Coordinates. The Academic Press, London. https://doi.org/10.1016/b978-0-12-547620-1.50007-2.

Pellow, S., Chopin, P., File, S.E., Briley, M., 1985. Validation of open:closed arm entries in an elevated plus-maze as a measure of anxiety in the rat. J. Neurosci. Methods 14, 149–167. https://doi.org/10.1016/0165-0270(85)90031-7.

Ramos-Miguel, A., Jones, A.A., Sawada, K., Barr, A.M., Bayer, T.A., Falkai, P., Leurgans, S.E., Schneider, J.A., Bennett, D.A., Honer, W.G., 2018. Frontotemporal dysregulation of the SNARE protein interactome is associated with faster cognitive decline in old age. Neurobiol. Dis. 114, 31–44. https://doi.org/10.1016/j.nbd.2018.02.006.

Reynaert, M.L., Marrocco, J., Mairesse, J., Lionetto, L., Simmaco, M., Deruyter, L., Allorge, D., Moles, A., Pittaluga, A., Maccari, S., Morley-Fletcher, S., Van Camp, G., Nicoletti, F., 2016. Hedonic sensitivity to natural rewards is affected by prenatal stress in a sex-dependent manner. Addiction Biol. 21, 1072–1085. https://doi.org/10.1111/adb.12270.

Son, G.H., Geum, D., Chung, S., Kim, E.J., Jo, J.H., Kim, C.M., Lee, K.H., Kim, H., Choi, S., Kim, H.T., Lee, C.J., Kim, K., 2006. Maternal stress produces learning deficits associated with impairment of NMDA receptor-mediated synaptic plasticity. J. Neurosci. 26, 3309–3318. https://doi.org/10.1523/jneurosci.3850-05.2006.

Sugama, S., Sekiyama, K., Kodama, T., Takamatsu, Y., Takenouchi, T., Hashimoto, M., Bruno, C., Kakinuma, Y., 2016. Chronic restraint stress triggers dopaminergic and noradrenergic neurodegeneration: possible role of chronic stress in the onset of Parkinson's disease. Brain Behav. Immun. 51, 39–46. https://doi.org/10.1016/j.bbi.2015.08.015.

Vallée, M., Maccari, S., Dellu, F., Simon, H., Le Moal, M., Mayo, W., 1999. Long-term effects of prenatal stress and postnatal handling on age-related glucocorticoid secretion and cognitive performance: a longitudinal study in the rat. Eur. J. Neurosci. 11, 2906–2916. https://doi.org/10.1046/j.1460-9568.1999.00705.x.

Wang, Y., Ma, Y., Hu, J., Zhang, X., Cheng, W., Jiang, H., Li, M., Ren, J., Zhang, X., Liu, M., Sun, A., Wang, Q., Li, X., 2016. Sex-specific effects of prenatal chronic mild stress on adult spatial learning capacity and regional glutamate receptor expression profiles. Exp. Neurol. 281, 66–80. https://doi.org/10.1016/j.expneurol.2016.04.016.

Yang, K., Jiang, X., Cheng, S., Bai, L., Xia, Y., Chen, C., Meng, P., Wang, J., Li, C., Tang, Q., Cao, X., Tu, B., 2019. Synaptic dopamine release is positively regulated by SNAP-25 that involves in benzo[a]pyrene-induced neurotoxicity. Chemosphere 237, 124378, 10.1016/j.

Zhang, X.H., Jia, N., Zhao, X.Y., Tang, G.K., Guan, L.X., Wang, D., Sun, H.L., Li, H., Zhu, Z.L., 2013. Involvement of pGluR1, EAAT2 and EAAT3 in offspring depression induced by prenatal stress. Neuroscience 250, 333–341. https://doi.org/10.1016/j.neuroscience.2013.04.031.